Available online at www.sciencedirect.com
SCIENCE DIRECT
Journal of Colloid and Interface Science 300 (2006) 105–110
JOURNAL OF Colloid and Interface Science
www.elsevier.com/locate/jcis

Interaction between poly(ethylene glycol) and two surfactants investigated by diffusion coefficient measurements

R. López-Esparza [a,*], M.-A. Guedeau-Boudeville [b], Y. Gambin [a], C. Rodríguez-Beas [c], A. Maldonado [d], W. Urbach [a]

[a] *Laboratoire de Physique Statistique, Ecole Normale Supérieure, 24 rue, Lhomond 75231, Paris, France*
[b] *Laboratoire de Physique de la Matière Condensée, MSC UMR 7057, Collège de France, Paris, France*
[c] *Posgrado en Materiales, Universidad de Sonora, 83000 Hermosillo, Sonora, Mexico*
[d] *Departamento de Física, Universidad de Sonora, 83000 Hermosillo, Sonora, Mexico*

Received 3 December 2005; accepted 28 March 2006

Available online 4 April 2006

Abstract

Dynamic light scattering (DLS) and fluorescence recovery after pattern photobleaching (FRAPP) were used to study the interaction of low molecular weight poly(ethylene glycol) (PEG) with micelles of two different surfactants: tetradecyldimethyl aminoxide (C_{14}DMAO, zwitterionic) and pentaethylene glycol *n*-dodecyl monoether ($C_{12}E_5$, non-ionic). By using an amphiphilic fluorescent probe or a fluorescent-labeled PEG molecule, FRAPP experiments allowed to follow the diffusion of the surfactant–polymer complex either by looking at the micelle diffusion or at the polymer diffusion. Experiments performed with both fluorescent probes gave the same diffusion coefficient showing that the micelles and the polymer form a complex in dilute solutions. Similar experiments showed that PEG interacts as well with pentaethylene glycol *n*-dodecyl monoether ($C_{12}E_5$).

Keywords: Polymer–surfactant interactions; Poly(ethylene glycol); Dynamic light scattering; Fluorescence recovery after pattern photobleaching

1. Introduction

The interactions between surfactant phases and polymers have attracted great interest in the last years because of the applications of mixed surfactant–polymer systems [1–3]. Surfactants are relevant in processes such as detergency, wetting, foaming or emulsification, while polymers are used to control the viscosity of solutions. The mixed systems have properties differing from those of the pure components due to the complexation of the polymer with the surfactant.

It is well known that ionic surfactants interact much more strongly than non-ionic surfactants with neutral polymers [1]. In fact, anionic surfactants have a higher affinity for neutral polymers than cationic surfactants [3]. Ionic surfactants form micellar complexes with the polymer chain, which are formed at the critical aggregation concentration (cac), which is substantially lower than the critical micellar concentration (cmc) of the pure surfactant solution.

In this paper, we study the interaction between the zwitterionic surfactant tetradecyldimethyl aminoxide (C_{14}DMAO) [4] and PEG. In our experimental conditions, C_{14}DMAO behaves like a non-ionic surfactant. The aim of the work is to know if C_{14}DMAO micelles and PEG molecules form complexes or if they remain as individual aggregates in solution since it has been shown that the addition of polymer to a lamellar phase induces a spontaneous formation of highly monodisperse multilayered vesicles [5]. In addition, we have performed similar experiments with PEG–$C_{12}E_5$ mixtures.

2. Materials and methods

Tetradecyldimethyl aminoxide (C_{14}DMAO) which was recrystallized twice, was a gift from Dr. H. Hoffmann. It is a zwitterionic surfactant but behaves like a non-ionic in neutral or al-

* Corresponding author.
E-mail address: lopez@lps.ens.fr (R. López-Esparza).

0021-9797/$ – see front matter
doi:10.1016/j.jcis.2006.03.071

kaline solutions as in our case [4]. Fluorescein-5-isothiocyanate (FITC 'Isomer I') was purchased from Molecular Probes.

Pentaethylene glycol *n*-dodecyl monoether ($C_{12}E_5$) was purchased from Nilkko Chemicals (Tokyo, Japan) and used as received.

Poly(ethylene glycol) (PEG) of molecular weight 20,000 g/mol and 5-(4,6-dichloro-*s*-triazin-2-ylamino) fluorescein hydrochloride, ($C_{23}H_{12}Cl_2N_4O_5HCl$ or Cl DTAF) were purchased from Sigma and used as received.

All samples were prepared in ultra-purified water (resistivity ≈ 18 MΩ cm).

2.1. PEG 20,000 labeling with DTAF

In order to follow the polymer diffusion with the FRAPP technique, we labeled PEG molecules with a fluorescent dye, according to the DTAF labeling of dextran [6]. In the following paragraph, we briefly describe the labeling procedure, which is represented in Fig. 1. Materials, synthesis details, and purification steps are described in details in Supplementary material. Numbers and letters between brackets refer to the synthesis steps depicted in Fig. 1.

2.2. PEG-propylamine (2)

The addition of bromopropylamine (a) (1 g) to a solution of PEG 20,000 (1) (1 g) in aqueous NaOH (6.2 N) gave 1.99 g of crude product. After dialysis against water, the product was lyophilized to afford 853 mg of white powder, PEG-propylamine (2).

2.3. PEG-propylamino-DTAF (3) and (4)

400 mg of PEG-propylamine (2) and Cl DTAF (b) (90 mg, 1.70×10^{-4} moles, i.e., 4.25 eq/NH_2) were allowed to react in sodium tetraborate buffer solution (0.1 M, pH 9) at room temperature overnight. The reaction mixture was dialyzed against Millipore water and lyophilized to afford 390 mg of yellow powder, crude dyed polymer (2b).

105.5 mg of crude dyed polymer (2b) were dissolved in aqueous NaOH (70 ml, pH 9) and dialyzed against 2 L of a NaOH (pH 9) solution for one month.

The dialyzed dyed polymer in solution was purified by gel exclusion chromatography and recovered in 3 elution volumes: A and B, orange solutions of dyed polymer PEG–DTAF, then C, yellow solution of free dye DTAF.

Solutions A and B were lyophilized to afford respectively 47.9 mg and 34.8 mg of a mixture of PEG di DTAF (3) and PEG mono DTAF (4).

In the following, only the fluorescent-labeled PEG from A will be used, called FPEG.

2.4. Dynamic light scattering (DLS)

In a dynamic light scattering experiment, a laser beam is scattered by a small volume of the sample; light is collected

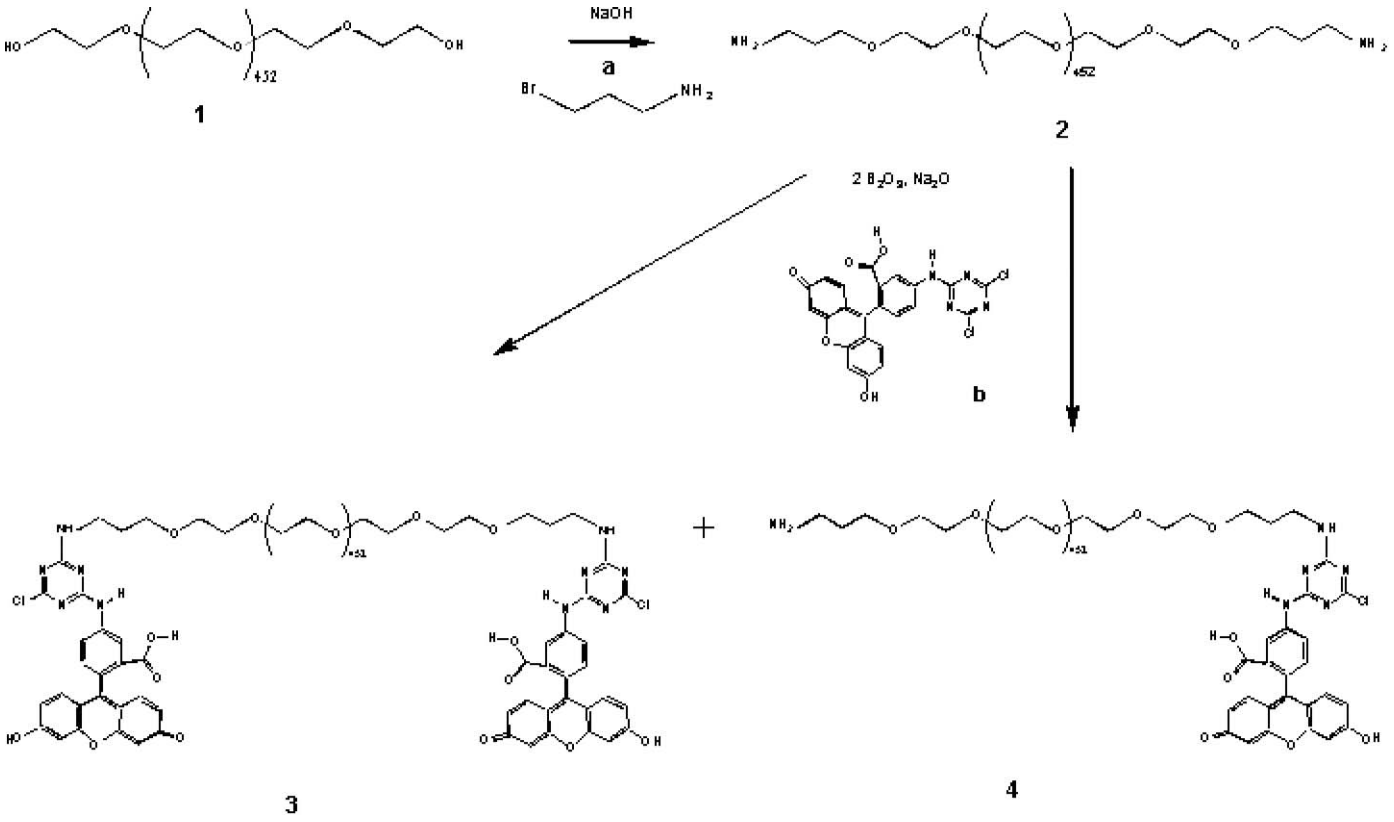

Fig. 1. Steps in the labeling procedure of PEG with a fluorescent molecule (DTAF) in order to obtain FPEG.

by a photomultiplier at an angle θ, with respect to the incident beam. The scattered light presents intensity fluctuations that can be related to the mutual diffusion coefficient D_m of the particles present in solution.

The normalized time autocorrelation function of the intensity of the scattered light for a given delay time τ is

$$g_2(\tau) - 1 = \beta\left|g_1(\tau)\right|^2, \quad (1)$$

where β is a factor that depends on the experimental geometry.

For monodisperse particles in solution the field correlation function decays exponentially, $g_1(\tau) = \exp(-\Gamma t)$, with a decay rate $\Gamma = D_m q^2$, where D_m is the mutual diffusion coefficient and $q = \frac{4\pi}{\lambda}\sin(\theta/2)$ is the magnitude of the scattering vector, λ and θ being the wavelength and scattering angle in the medium, respectively.

DLS experiments were performed in the homodyne mode using a 633 nm He–Ne laser and an ITI FW130 photomultiplier as light detector. The signal was digitized by an ALV-PM-PD amplifier-discriminator. The signal analyzer was an ALV-5000 digital multiple-τ correlator. The intensity autocorrelation function was measured at 50°, 70°, 90°, and 110°. The sample cells were 10-mL cylindrical ampules immersed in an index-matching bath of toluene, thermostated at 20 ± 0.1 °C.

2.5. Fluorescence recovery after pattern photobleaching (FRAPP)

The FRAPP technique has been described in detail elsewhere [7]. Briefly, a fluorescent probe is homogeneously dissolved in the sample, and an irreversible bleaching of the fluorescent groups is induced by a very brief powerful laser pulse. A less powerful laser beam is used to monitor the fluorescence signal as diffusion of the probes leads to a new homogeneous concentration in the illuminated region of the sample. We used a Spectra Physics argon laser (400 mW at 488 nm) for the photobleaching pulse; the weaker beam has a 1000 times lower intensity. Both the bleaching and the monitoring beams are divided and superposed in the sample to create an interference fringe pattern. After the bleaching pulse, a piezoelectric crystal makes the monitoring beam sweep the bleached fringes in the sample, which reduces the noise to signal ratio in the recovery exponential signal. The self-diffusion coefficients D_s are deduced from the characteristic times τ of the recovery curves by the classical relation $D_s = \frac{i^2}{4\pi^2\tau}$, where the interfringe values i are in the range 10–100 μm and the typical time values are from 0.1 to 10 s. The D_s values fitted to the above relation are obtained with an error smaller than 5%. FRAPP experiments were performed at 20 ± 0.1 °C.

2.5.1. Mutual vs self-diffusion

In the dilute regime, the mutual and the self-diffusion coefficients extrapolate to the same value. For spherical particles, a hydrodynamic radius R_H can be extracted using the Stokes–Einstein expression:

$$D = \frac{k_B T}{6\pi\eta R_H}, \quad (2)$$

where k_B is Boltzmann's constant, T is the temperature, and η is the viscosity of the solvent.

3. Results and discussion

3.1. Separate characterization of PEG and FPEG

We measured diffusion coefficients D_m of PEG by DLS (Fig. 2). The extrapolation of D_m for infinite dilution leads to a hydrodynamic radius of 2.61 ± 0.2 nm.

We have also determined by FRAPP the size of FPEG. The fluorescence recovery signal in all the experiments was monoexponential, that is, only diffusing particles of one size are detected, and no free-DTAF was observed. In Fig. 2 we plot the self-diffusion coefficient D_{FPEG} of the fluorescent polymer as a function of PEG concentration. The hydrodynamic radius of FPEG extrapolated to infinite dilution is 2.68 ± 0.2 nm is in good agreement with previously reported values [8,9] and with our DLS results for PEG.

These experimental values are also in good agreement with theoretical predictions. The gyration radius R_g for an ideal chain in a good solvent is related to the mean square end-to-end radius r by [10]

$$R_g \approx \frac{r}{\sqrt{6}},$$

where $r = 750 \times 10^{-4}(M)^{1/2}$ nm for PEG [9]. M is the molecular weight. For a Gaussian coil, the hydrodynamic radius R_H is approximately two-thirds of the radius of gyration [11,12]. Then

$$R_H = \frac{R_g}{1.5}.$$

Taking $M = 20{,}000$ g/mol, we find $R_H = 2.9 \pm 0.1$ nm, a value reasonably close to the DLS and FRAPP results. The negative

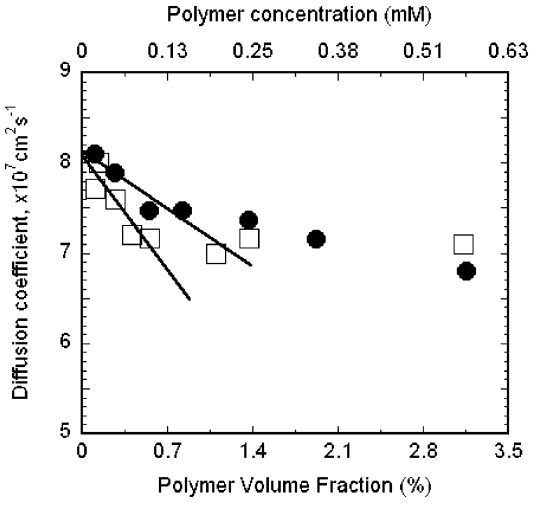

Fig. 2. Diffusion coefficient of PEG as measured with DLS (●). Self-diffusion coefficient D_{FPEG} of the fluorescent polymer measured using FRAPP (□). The lines are the fits from which the hydrodynamic radii of the polymers were obtained. (2.61 ± 0.2 nm for DLS and 2.68 ± 0.2 nm for FRAPP.) In all plots, the typical error is smaller than the symbol size.

slope of the diffusion coefficient curves indicates an attractive interaction between PEG molecules. This result agrees with the fact that PEG has a slight tendency to aggregate in solution [13].

3.2. C_{14}DMAO–PEG interactions

The surfactant concentrations studied are in the range $1 < c < 55$ mM. These concentrations are well above the critical micellar concentration (cmc = 0.12 mM at 25 °C). For concentrations c below ∼10 mM, the micelles are spherical. Electric birefringence experiments show that an increasing surfactant concentration leads to a sphere-to-rod transition at around 10 mM [4]. Small-angle neutron scattering experiments (SANS) confirm the existence of cylindrical micelles for the higher surfactant concentrations [14]. The polydispersity index obtained by this technique is in the range 0.4–0.8 [14].

3.2.1. DLS

In Fig. 3 we plot the diffusion coefficients obtained with DLS; all correlation functions were single exponentials. For each concentration, the polydispersity index obtained from cumulant fits to the DLS data was low (<0.5).

[PEG] = 0 mM The diffusion coefficient of the pure C_{14}DMAO micelles decreases from a value of 7.5×10^{-7} cm^2/s down to 3.5×10^{-7} cm^2/s, as the surfactant concentration is increased. Note that the surfactant volume fraction is small enough to neglect interactions between micelles, i.e., the variation in the diffusion coefficient is due to micelle growth.

[PEG] = 0.25 mM When PEG is added to the surfactant solution, the most diluted micelles see their diffusion coefficient hindered by a factor 1.7. As only one size is detected in solution, this suggests a formation of PEG–micelles complexes.

3.2.2. FRAPP

FRAPP experiments allow us to have insight on this C_{14}DMAO–PEG complex formation (Fig. 4).

[PEG] = 0 mM We have performed FRAPP experiments with pure C_{14}DMAO solutions for the same surfactant concentrations as in Fig. 3. The amphiphilic fluorescent probe used in these experiments is the fluorescein derivative, FITC grafted to a 12 carbon hydrophobic tail that anchors in the micelles. Thus, we follow the diffusion of the micelles in the system. As shown in Fig. 4 (●), the self-diffusion coefficients of the C_{14}DMAO micelles confirm the DLS results.

[PEG] = 0.25 mM The FRAPP technique allowed us to follow the two components of the mixed polymer–surfactant samples. When the amphiphilic probe was used, we followed the diffusion of the surfactant aggregates, whereas when the fluorescent polymer was used, we followed the diffusion of the polymer chains.

From Fig. 4 we can see that the self-diffusion coefficient measured for the amphiphilic fluorescent probe in these samples correspond to that found by DLS for this polymer concentration. In addition, the D values of the fluorescent-labeled

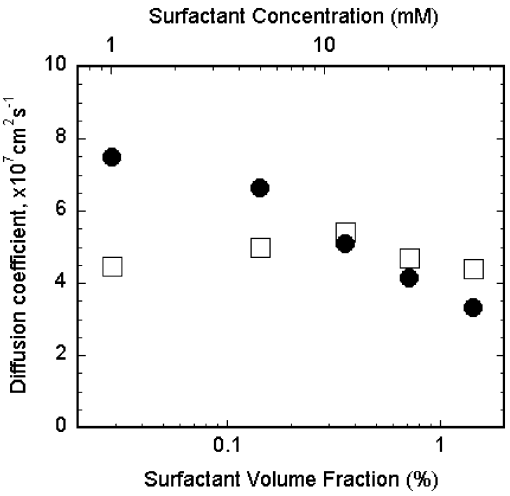

Fig. 3. DLS. Diffusion coefficients D plotted versus C_{14}DMAO concentration; $C_{PEG} = 0$ mM (●) and $C_{PEG} = 0.25$ mM (□). The surfactant volume fraction was calculated using $\rho_{C_{14}DMAO} = 0.89$ g cm^{-3}.

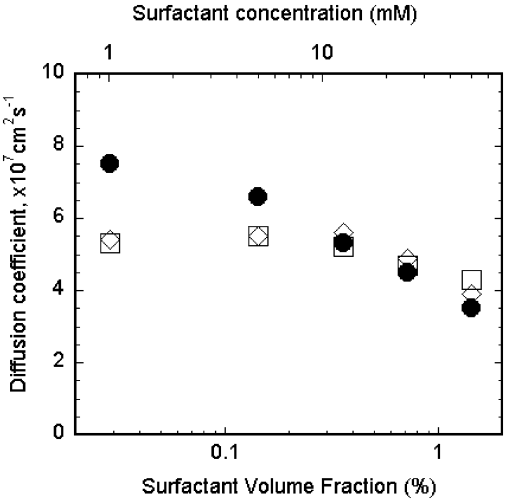

Fig. 4. FRAPP. Plot of self-diffusion coefficients D versus C_{14}DMAO concentration. Micelles were labeled with the fluorescent amphiphilic probe C_{12}-FITC. Concentrations as in Fig. 3, $C_{PEG} = 0$ mM (●) and $C_{PEG} = 0.25$ mM (□). The fluorescent-labeled FPEG (◇) ([FPEG] = 0.05 mM and [PEG] = 0.20 mM) have the same mobility than the micelles.

FPEG (◇) are identical to the values found for the amphiphilic probe (□). At low surfactant concentrations, the diffusion coefficients associated with both the surfactant micelles and the fluorescent polymer have the same value, significantly smaller than that obtained for pure surfactant micelles (●).

This adds information on the DLS results, clearly demonstrating the formation of a polymer–surfactant complex.

Note that for the highest surfactant concentrations, the polymer–surfactant complex mobility is faster than that of the pure surfactant micelles. This result comes from the fact that below 10 mM, the pure surfactant micelles are spherical, while above 10 mM, they are cylindrical [4,14]. The growth and the change of shape of the micelles explain the variation of their mobility, as a function of surfactant concentration, in the pure surfactant system. Obviously, the polymer modifies these

micellar transformations, and the diffusion coefficient of the complex has a less-pronounced variation.

The interaction between C_{14}DMAO and PEG is probably of hydrophobic type. In fact, earlier work, based on NMR experiments suggests this kind of interactions for PEO and ionic surfactants [15,16]. In addition, our results agree with the continuous adsorption mechanism found in computer simulations for systems where the binding between polymer and surfactant is dominated by hydrophobic interaction (i.e., when the surfactant tails tend to adsorb on the polymer) [17].

3.3. $C_{12}E_5$–PEG system

3.3.1. DLS

[PEG] = 0 mM We performed DLS experiments with polymer-free $C_{12}E_5$ micelles in samples with surfactant concentrations in the range 1 mM $\leqslant c \leqslant$ 90 mM. The critical micellar concentration of $C_{12}E_5$ at 25 °C is 65 μM [18]. The clouding temperature of the binary system $C_{12}E_5$–water is around 31 °C [19]. Micelles are cylindrical and polydisperse for all concentrations [20,21].

The DLS correlation functions are unimodal for surfactant concentrations $\leqslant$5 mM. The relaxation time (τ) is linearly dependent on q^{-2} demonstrating a diffusive process.

For surfactant concentrations $\geqslant$5 mM the correlation function is very close to a single exponential, although a small-amplitude, non-diffusive, faster component appears (less than 10% of total signal intensity). This component was not detected by FRAPP experiments, and will not be taken into account hereafter. More experiments are necessary to clarify the origin of this component.

The measured diffusion coefficients are plotted in Fig. 5 where the filled circles represent values obtained from the single exponentials ($c \leqslant$ 5 mM) and from the slow modes ($c \geqslant$ 5 mM).

The D values obtained are smaller than those found for C_{14}DMAO, indicating larger micelles. The behavior observed agrees with results reported for this concentration range, for the single exponential correlation functions and for the slow modes [21].

[PEG] = 0.25 mM When PEG is added to the $C_{12}E_5$ solutions, the DLS correlation functions become bimodal for $[C_{12}E_5] < 5$ mM, the two characteristic times corresponding to diffusive processes. The diffusion coefficients obtained are plotted in Fig. 5.

For low surfactant concentrations, the diffusion coefficient associated with the fast mode is very close to that of free PEG (horizontal broken line in Fig. 5, as calculated from the data in Fig. 2). The slow mode in the polymer–surfactant samples yields diffusion coefficients very similar to those of the polymer-free micelles.

However, by increasing the concentration of surfactant, a more dramatic effect appears as shown in Fig. 5. The D values corresponding to the fast mode start to decrease from $[C_{12}E_5] = 8$ mM, down to the slow mode D values (attained for $[C_{12}E_5] \approx 10$ mM).

In order to determine the localization of the PEG molecule and detect possible PEG–$C_{12}E_5$ complexes, we used the complementary FRAPP experiments (Fig. 6).

3.3.2. FRAPP

[PEG] = 0 mM We have performed FRAPP experiments with pure $C_{12}E_5$ solutions for the same surfactant concentrations as in Fig. 5; the data (●, Fig. 6) obtained correspond well to the DLS results.

[PEG] = 0.25 mM When non-fluorescent PEG is added to the micelles labeled with C_{12}-FITC, the diffusion coefficients obtained (△) exhibit a monotonic evolution similar to the one observed for PEG-free micelles (●). For $c < 8$ mM, the higher

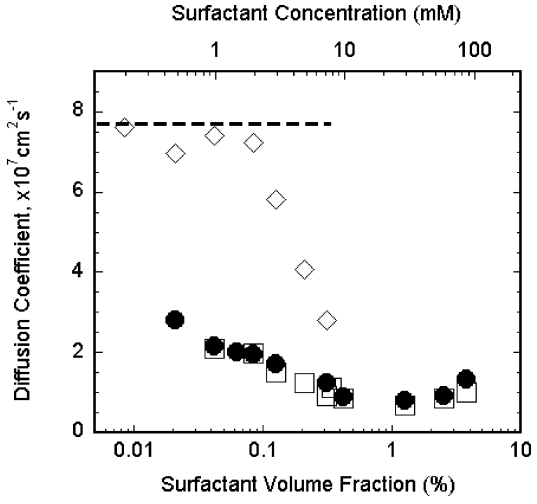

Fig. 5. Diffusion coefficients obtained from DLS experiments for $C_{12}E_5$ micelles as a function of surfactant concentration (●). Slow (□) and fast (◇) modes obtained from DLS for PEG–$C_{12}E_5$ samples ([PEG] = 0.25 mM). The broken line represents the diffusion coefficient of PEG in pure water.

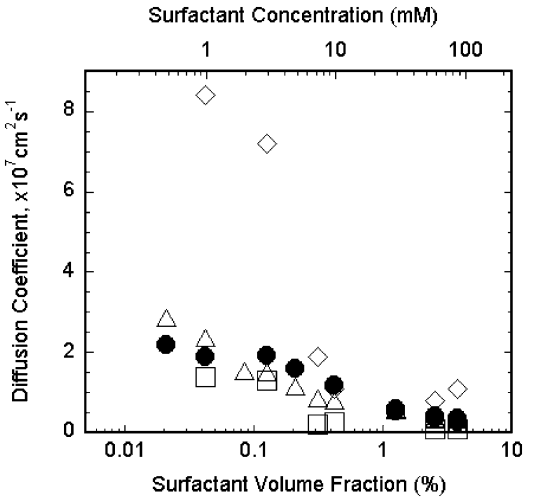

Fig. 6. FRAPP. Diffusion coefficients D versus $C_{12}E_5$ concentration, for polymer-free micelles (●) and for micelles in the presence of 0.25 mM PEG (△). The micelles were labeled with C_{12}-FITC. Two D values are detected when using FPEG (◇ and □, respectively).

D values obtained by DLS are not detected, suggesting that the small aggregates are not micelle-like objects.

For $[C_{12}E_5] < 8$ mM, using fluorescent-labeled FPEG, the fluorescence recovery curves are perfectly fitted by a two-exponential expression:

$$\Delta I(t) = C_1 + C_2 e^{-t/\tau_1} + C_3 e^{-t/\tau_2}. \quad (3)$$

Both characteristic times define Brownian motion by scaling as q^2. The corresponding D values correspond to the two values found by DLS (Fig. 5).

The faster mode is thus due to PEG molecules that do not interact with micelles, the slower mode corresponds to PEG–micelles complexes.

For $[C_{12}E_5] > 10$ mM, the data clearly indicate that all PEG molecules form complexes with micelles.

Although surprising, this result agrees with data obtained for higher molecular weight PEG [19]. For low surfactant concentrations the observed diffusion modes (Figs. 5 and 6) are related to PEG–$C_{12}E_5$ complexes and PEG molecules (without surfactant). This effect is probably due to the fact that the surfactant does not adsorb molecule by molecule onto the polymer. Instead, entire surfactant micelles adsorb onto individual polymer molecules. As the aggregation number of $C_{12}E_5$ is >100 [21,22], when the surfactant concentration is low, there are no enough micelles available for adsorption to every PEG molecule. This result agrees with the generally accepted picture where complete surfactant micelles adsorb on the polymer, leading to a necklace of micelle pearls on a polymer backbone [23]. Computer simulations predict this kind of adsorption when the binding between polymer and surfactant is dominated by the surfactant headgroups [17].

4. Conclusions

We have studied the interaction between a hydrosoluble polymer (PEG, $M_w = 20{,}000$ g/mol) and the micelles of two different surfactants. Our experimental results show that the polymer interacts with C_{14}DMAO (a zwitterionic surfactant which behaves like a non-ionic one in our experimental conditions) forming a polymer–surfactant complex. This conclusion agrees with preliminary results obtained with the same polymer but different lyotropic phases (lamellar, sponge) of the same surfactant [5]. The interaction between PEG and C_{14}DMAO seems to be of hydrophobic type. The DLS and FRAPP experiments show in the same manner that PEG interacts with $C_{12}E_5$. Since the polar head of the surfactant is a PEG motif, this is rather an unexpected result. The PEG–$C_{12}E_5$ interaction is due to the binding of the polymer and the surfactant polar head.

Acknowledgments

The authors are grateful to M. Waks for critical reading of the manuscript. The authors thank the financial support from ECOS-Nord and ANUIES (action MOOP03). R.L.-E. acknowledges a scholarship from the Consejo Nacional de Ciencia y Tecnología (Conacyt-Mexico). A.M. thanks financial support from Conacyt-Mexico (Grant on "Materiales Biomoleculares" 074).

Supplementary material

The online version of this article contains additional supplementary material.

Please visit DOI: 10.1016/j.jcis.2006.03.071.

References

[1] E.D. Goddard, K.P. Ananthapadmanabhan (Eds.), Interactions of Surfactants with Polymers and Proteins, CRC Press, 1993.
[2] J.C.T. Kwak (Ed.), Polymer–Surfactant Systems, Dekker, New York, 1998.
[3] K. Holmberg, B. Jönsson, B. Kronberg, B. Lindman, Surfactants and Polymers in Aqueous Solution, second ed., Wiley, 1998.
[4] H. Hoffman, G. Oetter, B. Schwandner, Prog. Colloid Polym. Sci. 73 (1987) 95.
[5] A. Maldonado, R. López-Esparza, T. Gulik-Krzywicki, W. Urbach, C. Williams, J. Colloid Interface Sci. 296 (1) (2006) 365.
[6] S. Prigent-Richard, M. Cansell, J. Vassy, A. Viron, E. Puvion, J. Jozefonvicz, D. Letourneur, J. Biomed. Mater. Res. 40 (2) (1998) 275.
[7] D. Chatenay, W. Urbach, C. Nicot, M. Vacher, M. Waks, J. Phys. Chem. 91 (1987) 2198.
[8] M.F. Ficheux, A.M. Bellocq, F. Nallet, J. Phys. II France 5 (1995) 823.
[9] J. Brandrup, E.H. Immergut, E.A. Grulke (Eds.), Polymer Handbook, fourth ed., Wiley & Sons, 1999.
[10] H. Yamakawa, Modern Theory of Polymer Solutions, Harper and Row, New York, 1971.
[11] M. Schmidt, W. Burchard, Macromolecules 14 (1981) 210.
[12] S. Park, T. Chang, Macromolecules 24 (1991) 5729, and references therein.
[13] J. Israelachvili, Proc. Natl. Acad. Sci. USA 94 (1997) 8378.
[14] N. Gorski, J. Kalus, J. Phys. Chem. B 101 (1997) 4390.
[15] Z. Gao, R.E. Wasylishen, J.C.T. Kwak, J. Colloid Interface Sci. 137 (1990) 137.
[16] Z. Gao, R.E. Wasylishen, J.C.T. Kwak, J. Phys. Chem. 95 (1991) 462.
[17] (a) R.D. Groot, Langmuir 16 (19) (2000) 7493–7502;
(b) C. Thunig, H. Hoffmann, G. Platz, Prog. Colloid Polym. Sci. 79 (1989) 297.
[18] C. Sin, D. Woermann, Ber. Bunsenges. Phys. Chem. 96 (7) (1992) 913.
[19] M. Corti, C. Minero, V. Degiorgio, J. Phys. Chem. 88 (2) (1984) 309.
[20] W. Brown, Z. Pu, R. Rymdén, J. Phys. Chem. 92 (1988) 6086.
[21] E. Feitosa, W. Brown, P. Hansson, Macromolecules 29 (1996) 2169.
[22] E. Feitosa, W. Brown, M. Vasilescu, M. Swanson-Vethamutu, Macromolecules 29 (1996) 6837.
[23] B. Cabane, J. Phys. Chem. 81 (17) (1977).